Combined Optical and Neural Network Fingerprint Matching

C L. Wilson, C. I. Watson, and E. G. Paek,
Information Technology Laboratory,
National Institute of Standards and Technology
Gaithersburg, MD 20899

Abstract

This paper presents results on direct optical matching of inked and real-time fingerprint images. Direct optical correlations and hybrid optical neural network correlation are used in the matching system for inked fingerprints. Preliminary results on optical correlation matching of real-time fingerprints. The test samples used in the inked image experiments are the fingerprint taken from NIST Special Database SD-9. These images, in both binary and gray level forms, are stored in a VanderLugt correlator [1]. Tests of typical cross correlations and auto correlation sensitivity for both binary and 8 bit gray images are presented. When global correlations are tested on a second inked image results are found to be strongly influenced by plastic distortion of the finger. When the correlations are used to generate features that are localized to parts of each fingerprint and combined using a neural network classification network and separate class-by-class matching networks, 91.1% matching accuracy is obtained on a test set of 100,000 image pairs. Initial results with real-time images suggest that the difficulties resulting from finger deformation can be avoided by combining many different distorted images when the hologram is constructed in the correlator. Testing this process will require analysis of 10-20 second sequences of digital video.

1 Introduction

This paper presents data on two types of fingerprint images and two types of correlators. The two types of fingerprint images are rolled inked prints scanned at 20 pixels/mm scan rate and real-time fingerprint images acquired using NTSC video from an real-time optical live scan device. We study matching of the inked fingerprints using global optical correlations [1] and partial optical correlation features and a system of neural classification and matching networks [2].

Initial results for live scan prints (real-time data) and static rolled inked fingerprints for optical matching show that, with proper selection of input for the stored hologram, direct optical matching of live scanned fingerprints is reliable. This reliability is maintained so long as the sample of live scan prints contains small variations in rotations and variations in pressure during the 10-second hologram exposure. When a single static live scan image is

used, optical matching has lower reliability in that the user must move their finger until a position and level of ridge distortion which matches the hologram is found. This is because the match in the static image case only occurs when the finger position and distortion closely match the image used to expose the hologram.

In the inked rolled fingerprint case, even after core alignment and correction for rotation, optical matching of most prints is sucessful for matching the original image and rejecting other fingerprints but fails on second copies of rolled images because plastic pressure distortions and image size variation are too large to allow global matching. Detailed computer simulations show that global optical matching uses the fine grained phase plane structure of the Fourier transform of the fingerprints to produce strong optical correlations. This fine grained structure is sensitive to pressure and image size effects which then dominant in correlations of static fingerprints.

The fine grained local variations in fingerprints can be partially compensated for by calculating optical correlations on smaller zones of the fingerprints. A training set was derived from volume two of SD-9 and the testing set from volume one of SD-9 [3]. In our experiments, two four by four matrices of correlations on zones of the fingerprint are used to produce a total of 64 features. One set of correlations is computed with the local zone grid centered on the core and one set is computed with the core in the center of the grid just above and to the left of grid center.

These features are combined using two types of neural networks. The first network is used to classify the fingerprints [4, 5, 6]. After each fingerprint is classified, class-by-class matching networks are trained for each class. These two networks function in a way similar to the binary decision networks discussed in [7]. For this particular problem, the network training is strongly dependent of regularization and pruning for accurate generalization [2].

Section 2 describes the direct optical correlation experiment. In section 3 we discuss combining optical and neural network methods. Section 4 we discuss some initial results for real time fingerprints. In section 5 we draw some conclusions about the difference in correlations of real time and rolled inked fingerprints.

2 Global Optical Correlations

In the global optical matching experiment images from NIST special data base 9 (SD-9) [3] are core aligned using the method discussed in [4] and cropped to fit the 640 by 480 pixel field of the pattern recognition system. One hundred reference fingerprints and second rollings (inked images taken at a different time) are available for auto correlation and cross correlation experiments. When binary finger prints are used the method of used is based on that presented in [5].

Figure 1 shows a schematic diagram of the optical pattern recognition system. It is based on the conventional VanderLugt correlator [1]. The target fingerprint image is loaded on an SLM and is Fourier transformed by a lens. The resulting Fourier spectrum is interfered with a reference beam to record a Fourier transform hologram. After recording is finished, if an arbitrary input fingerprint is presented on the SLM, the correlation of the input and the target appears in the correlation output plane.

Although the spatial heterodyning technique, often called joint transform correlator [8], has many advantages for real-time applications [9, 10] and was used in most of recent fingerprint recognition experiments [11, 12, 13, 14, 15, 16], the VanderLugt correlator was adopted

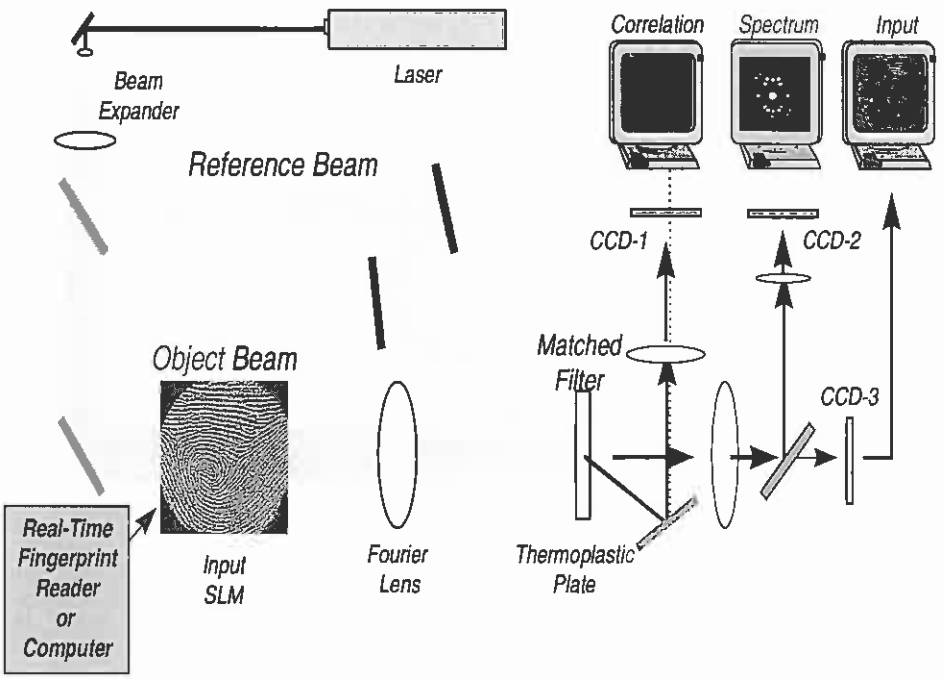

Figure 1: Diagram of the optical pattern recognition system

in this experiment. This is because the VanderLugt correlator does not require a fast SLM with high resolution and the large SBP (space bandwidth product) available from holographic recording materials provide high degree of freedom to accommodate various distorted versions of a target that are simultaneously compared with an input. Also, since the information is recorded in the form of a diffraction pattern (hologram) instead of a direct image, it can be used on a cridit card or an ID card for security purposes without need for further encoding. Finally, the VanderLugt correlator is better suited for spatial filtering to increase signal to noise ratio (SNR). The critical positioning tolerance problem of the VanderLugt correlator can be greatly relaxed by using in-situ recording materials such as thermoplastic plates as were used in this experiment. In this case, once the system is aligned, new holographic filters can be generated with no fear of misalignment.

In the global correlation experiment, fingerprint images are generated from the NIST fingerprint database [3]. In the real time correlation experiment images are generated by a live-scan fingerprint scanner (Identicator Technology, Gatekey Plus ver. 4.1) [1]. An electrically addressable liquid crystal spatial light modulator (Kopin, LVGA kit, 14 mm diagonal)[1] is used as an input device. The SLM is mounted on a rotational stage to facilitate precise rotational tolerance measurements.

[1]Certain commercial equipment may be identified in order to adequately specify or describe the subject matter of this work. In no case does such identification imply recommendation or endorsement by the National Institute of Standards and Technology, nor does it imply that the equipment identified is necessarily the best available for the purpose.

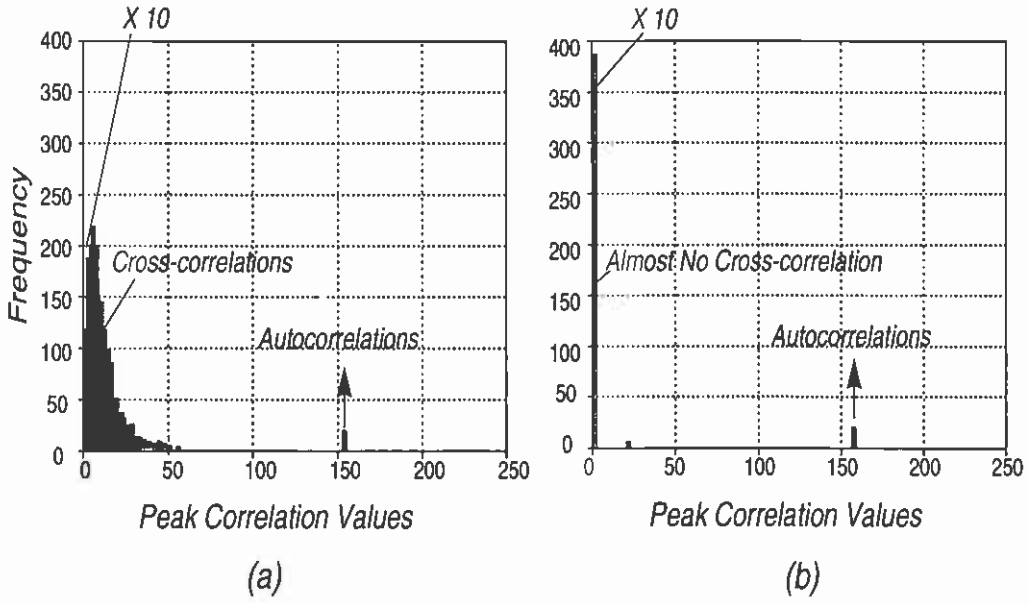

Figure 2: Histograms of peak correlations for gray (a) and binary (b) fingerprint images.

Holographic filters are recorded on a thermoplastic plate (Newport Corp. HC-300)[1] that allows a fast non-chemical processing, high diffraction efficiency and high responsibility. Although the recording process cannot be achieved in real-time (close to 1 minute), the time-consuming comparison of an input with many other images in a large database can be done very fast, once a hologram is made.

A 10 mW HeNe laser with a ND 2 filter was used as a light source, so only 0.1 mW is used to see correlation output due to the high light efficiency of the system.

The system is also equipped with the real-time in-situ monitoring of an input image, its Fourier transform, and the correlation output. These monitoring parts, combined with a frame grabber and other analytic tools, permit real-time quantitative analyses and accurate characterization of every stage of the system operation.

The correlator system is capable of shift-invariant pattern recognition over a broad range of input positions and has high SNR due to accurate alignment using an interferometer and a microscope.

Figure 2 shows a histogram of peak correlations for gray (a) and binary inputs (b). For each of 20 randomly chosen fingerprints, a holographic filter was fabricated and tested against the 200 fingerprints in the NIST database. Therefore each plot involves 4,000 correlations. Each peak correlation value was obtained by taking the maximum value in the correlation plane. In case of gray inputs shown in (a), all 20 autocorrelations peak at the maximum value (152). Cross-correlations distribute in a Gaussian shape with a peak at 0, FWHM of around 15, and the maximum at 60.

For binary inputs shown in (b), all autocorrelations peak at the maximum value, as in gray inputs. However, in this case, cross-correlations are significantly reduced to zero except for the few cases which were found to be from the correct fingerprints obtained at different

Figure 3: Correlation of two rollings of the same print. (Dark gray indicates correlated ridges, white and light gray indicate uncorrelated ridges.)

times.

For both gray and binary inputs, autocorrelations are well separated from cross-correlations to permit perfect 100% recognition for correct fingerprints (without considering distortions).

The exact mechanism for the significant increase in SNR for binary inputs is not completely understood. However, several previous works [17, 18] support the experimental results. Such a high SNR of binary inputs can be efficiently used to make a composite filter to permit tolerance against distortion.

3 Combined Optical and Neural System

Direct global correlation of fingerprints for matching has a significant failure rate caused by the elasticity of fingerprints. Two rollings of the same print can vary significantly, as seen by computing their Fourier transforms, because of the stretching variations which occur when rolling a fingerprint. Figure 3 shows the correlation of two rollings of the same print that have been rotation and translation aligned based on the ridge structure around the core. It is clearly seen that the fingerprints correlate (indicated by the dark gray pixels) around the core but away from the core the patterns have different amounts of elastic distortion.

Since the elastic distortion problem is local, a method of local correlation can be used to lower the average distortion in small subregions of the fingerprint.

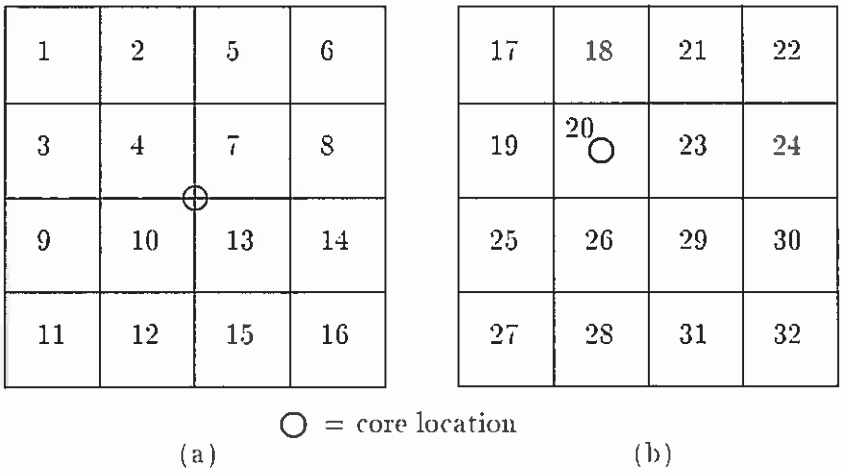

Figure 4: Shows image partitioning and the corresponding feature number.

3.1 Optical Features

A solution to the elastic distortion that occurs in different rollings of the same fingerprint is to partition the images into tiles and compare the data within each of the tiles using transform based methods. For this work, the image was partitioned into 4 by 4 tiles twice. One partition with the core located in the center of the image, as defined by the fingerprint core, and the second time with the core shifted away from the center to be in the center of a subimage. This double partitioning allowed for overlap of data (specifically data on the edge of the tiles). Since the neural network is allowed to prune any data that is not needed, excess overlap in the features can be removed during network training. Figures 4a-b show the core location for each 4x4 partition.

After partitioning, each f(n) and s(m) pair are compared by correlated the corresponding tiles (32 tiles) for each image and extracting features from the correlations as inputs to the neural network. The features used are the central correlation peak area and width. Figure 5 shows two image sections from a matched pair and the corresponding correlation output. The correlation peak is extracted by taking a cross-section (perpendicular to the ridge direction) of the peak at the maximum correlation value. Figure 6 shows some typical data for a matched pair with data of unmatched fingerprints. The distinguishing characteristic of the matched pair peak is that it has more dominant maximum and minumum data points and a narrower width.

The correlation is computed in the Fourier domain by taking the Fourier Transform of the partitions and computing the inverse Fourier Transform of their product, using the complex conjugate of the first (eq. 1).

$$f(n) \circ s(m) = \mathcal{F}^{-1}[\mathcal{F}^{*}[f(n)] \times \mathcal{F}[s(m)]] \tag{1}$$

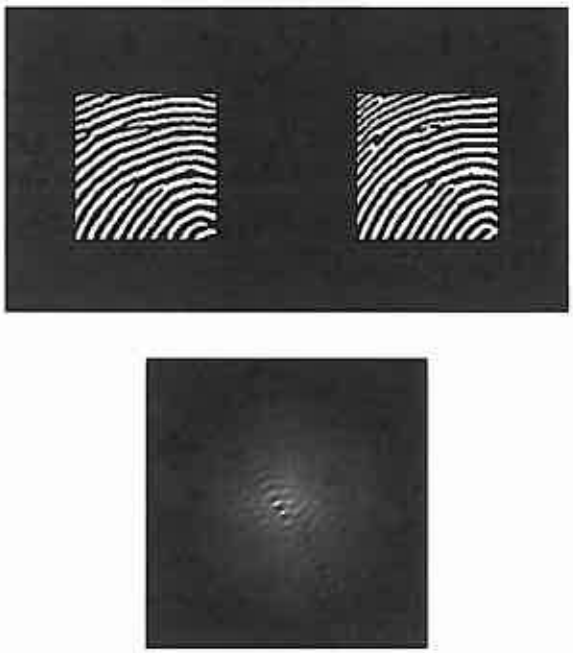

Figure 5: Original matched pair and corresponding correlation.

Each f(n) and s(m) input vector has 64 features (32 peak areas and 32 widths) (n = 1,2, ... 900 and m = 1,2, ... 900):

$$
\begin{array}{c}
peak\_features[f(n)_1 \circ s(m)_1] \\
peak\_features[f(n)_2 \circ s(m)_2] \\
\vdots \\
peak\_features[f(n)_{31} \circ s(m)_{31}] \\
peak\_features[f(n)_{32} \circ s(m)_{32}]
\end{array}
$$

The automated feature detection procedures were applied to NIST Special Database 9 Vol 1, where disk2 was used as training data and disk1 was used as testing data.

For this partitioning technique to be effective, the images need to be rotationally and translationally aligned about the cores of the two fingerprints being compared. This alignment was accomplish over a large set of data using an automated technique. There are three steps in the automated alignment, filter/binarize image, detect core location, and determine alignment.

Filtering, binarization, and core detection are done using methods previously developed and discussed in detail in [6]. The only addition is that the binarized fingerprint is median filtered using a 3 by 3 window to help smooth noise in the ridge data and improve correlation performance.

The final step uses 128 by 128 segments that are centered about the core of the fingerprints being aligned. The correlation of the segments is computed while rotating the second segment over a range of angles. The angle which produces the largest correlation is used for rotation alignment. Since two prints can have significant angular displacements the alignment is

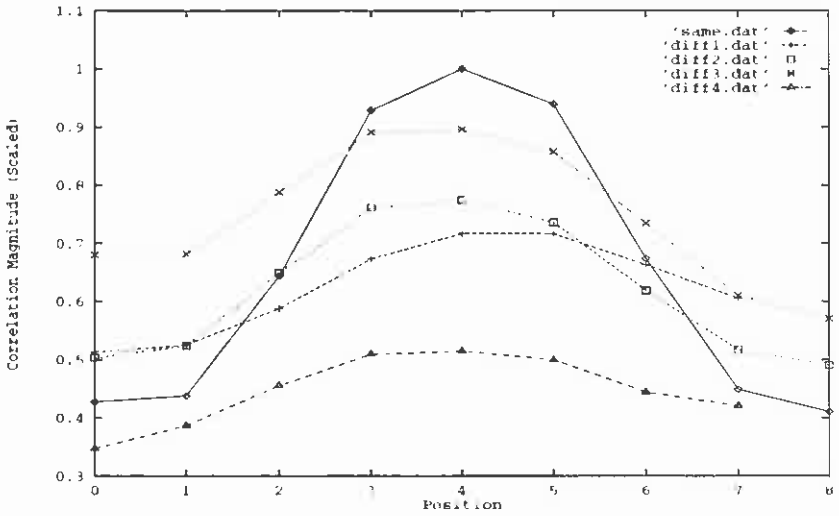

Figure 6: Plot of sample correlation peak data.

actually done in two stages. Stage one uses an angular step size of 1 degree over a range of +/- 15 degrees and stage two a step size of 0.2 degrees over a range of +/- 1 degree from the angle determined in the first stage.

Since the correlation computed by equation 1 is translation independent, translation alignment is accomplished by using the peak correlation location from the second stage of the angular alignment. The amount that the peak correlation is off center of the 128x128 segment determines how much the second print needs to be shifted to achieve translational alignment with the first.

This procedure results in 64 features for each pair of fingerprints that is compared. In SD-9, each finger print has one print in the test set that matches and several thousand which do not match. Only those prints which do not match but are of the same class are included in the training set. The previously developed neural network classifier [6] is used for this screening process.

3.2 Neural Network Matching

The matching networks discussed in this section were trained using a dynamically modified scaled conjugate gradient method presented in [2]. In [2], we demonstrated that performance equal to or better than Probabilistic Neural Network (PNN) [19] can be achieved with a single three-layer Mult-Layer Perceptron (MLP) by making fundamental changes in the network optimization strategy. These changes are: 1) Neuron activation functions are used which reduce the probability of singular Jacobians; 2) Successive regularization is used to constrain volume of the weight space being minimized; 3) Boltzmann pruning is used [20] to constrain the dimension of the weight space; and 4) Prior class probabilities are used to normalize all error calculations so that statistically significant samples of rare but important classes can be included without distortion of the error surface. All four of these changes are made in the inner loop of a conjugate gradient optimization iteration [21] and are intended to simplify the training dynamics of the optimization.

In this work we found that the effect of sinusoidal activation, 1 above, was not useful but that pruning, 3 above, and regularization, 2 above, were essential to good generalization.

Since the distribution of match and do not match classes was highly unequal, the effect of prior weights, 4 above, was also very important.

The 64 local features discussed section in 3.1 were separated into testing and training samples both by class and as a global (all class) set. The training sets were used to calculate global and by class covariance matrices and eigenvectors and to calculate 59 K-L transform [22] features for all of the testing and training sets. When the eigenvectors of the K-L transform were examined, the primary source of variation was found to be in 12 zones near the center of the two feature grids. The first eigenvector of each of the transforms was approximately 40 times larger than the 59th eigenvector indicating that only about 59 statistically independent features were computed from the training sets. No large difference in K-L transform characteristics were seen between global and class-by-class data sets.

The 59 component K-L transformed features were used to train neural networks for both global and class by class matching. The networks were trained using regularization to bound weight size and pruning to restrict the number of active weights in the network to a size. Network size, pruning, and regularization were adjusted empirically to provide reasonable generalization. The criterion used to test generalization accuracy was the comparison of the test and training matching errors.

3.3 Hybrid Results

The optimal regularization factor for all runs was found to be 0.001 and the optimum pruning temperature was found to be 0.005. The basic network size was 59-24-2 network with 1490 weights including bias weights. A sigmoidal activation function was used for the hidden nodes. With this network size and training parameters a typical functioning network has approximately 300 weights and has a accuracy of 74%-82%.

The results of this process are given in the table below.

Class	train	test	wts. pruned	total wts.	Test set size
All	78.3	76.0	1144	1442	258444
Arch	80.1	76.0	1135	1490	1681
Left Loop	82.2	84.9	1276	1466	73984
Right Loop	82.6	79.9	1251	1466	68121
Tented Arch	96.0	74.5	963	1490	1089
Whorl	84.8	82.7	1235	1490	113569

Table 1: Results of testing and training for global and class-by-class neural network matching using 58-28 K-L features. All class networks had 24 hidden nodes while the all network had 48 hidden nodes.

These results can be significantly improved by using PCASYS or some other classification method to test only prints of the same class for matching. Assuming the PCASYS accuracy of 99% correct classification at 10% rejects and a natural distribution of classes would allow the results given above to be improved to 91.1% matching accuracy. This model assumes that each print is classified or rejected by PCASYS. The rejected prints are matched with the All network given in the top line of the table. All other prints are matched by the

network selected by its PCASYS class. All prints misclassified by PCASYS are assumed to be mismatched.

The process of calculating the results shown in table 1 involved training runs in which both the regularization and pruning were systematically varied to determine the correct network size and the appropriate dynamics for training. As discussed in [20], network size in an indication of the amount of information that can be transferred between the training sample and the network without learning random noise patterns. In table 1, all of the final networks had a potential weight space size of 1490 weights. Larger networks were found to have poorer testing error than networks of this size. The pruning temperature was varied to produce similar testing and training errors for each class and for the global class. As the table shows this produced weight reductions of from 963 to 1276 weights. The small network size and large pruning ratio for acceptable generalization with training set of up to 100,000 samples shows that the noise in the features used in the training is at a level where larger network sizes are not useful because all of the information needed for generalization is learned by these small networks.

All of the pruning experiments require that some small amount of regularization be used to constrain the volume of weight space [2]. This allows the discriminant surfaces to remain in the part of the training space which is heavily populated by the data. All of these run were done in the 59 feature K-L space but numerous test pruning and regularization run were made in the original 64 feature space. Similar effective weight spaces were found in the full 64 feature space, about 300 weights. The 59 feature data set was selected for additional testing to save on computation time during training.

4 Real-Time Fingerprint Images

Preliminary testing on real time data show that problems with plastic distortion of fingerprints can be solved with careful construction of the hologram. Specifically, by constructing a composite hologram with a 10 second sequence of digital video input, where the individual makes small movements creating plastic distortions, matching works with global correlations. The method still has a small tolerance to rotation but is able to match multiple copies of the same print containing plastic distortions. More extensive testing of this procedure is planned using a larger data set.

5 Conclusions

We have compared optical and combined optical-neural network methods for rolled inked fingerprint image matching and optical correlation for matching of real-time fingerprint images. For static inked images direct global optical correlation of inked images made at different times has very low reliability although cross correlations and auto correlations of the original inked images are good. This difficulty can be accounted for by the plastic deformation of the fingerprint during rolling.

Combining zonal optical features with neural networks for classification and matching can yield reliable matching with an accuracy of 91.1%. The information content analysis of the features, both from the dimension of the K-L transform features and the generalization error analysis, show that the information transfer from the training data to the classification network is as high as the noise level of the features will allow. Under the conditions, further

improvement in the matching accuracy can only be achieved if the feature set information content is increased and the noise level is decreased.

Using real-time digital video input to create compostite holograms shows good results for dealing with plastic fingerprint distortions. Future studies in this area will be required to specify the details of proper hologram construction. Testing the composite hologram formation process will require analysis of 10-20 second sequences of digital video.

References

[1] A. VanderLugt. Signal detection by complex spatial filtering. *IEEE Trans. Inform. Theory*, IT-10:139–145, 1964.

[2] C. L. Wilson, P. J. Grother, and C. S. Barnes. Training Dynamics and Neural Network Performance. *Neural Networks*, to be published, 1997.

[3] C. I. Watson. Mated Fingerprint Card Pairs. Technical Report Special Database 9, **MFCP**, National Institute of Standards and Technology, February 1993.

[4] C. L. Wilson, G. T. Candela, P. J. Grother, C. I. Watson, and R. A. Wilkinson. Massively Parallel Neural Network Fingerprint Classification System. Technical Report NISTIR 4880, National Institute of Standards and Technology, July 1992.

[5] C. L. Wilson, G. T. Candela, and C. I. Watson. Neural-network fingerprint classification. *Journal of Artificial Neural Networks*, 1(2):203–228, 1994.

[6] G. T. Candela, P. J. Grother, C. I. Watson, R. A. Wilkinson, and C. L. Wilson. PCASYS - A Pattern-level Classification Automation System for Fingerprints. Technical Report NISTIR 5647, National Institute of Standards and Technology, 1995.

[7] C. L. Wilson, P. J. Grother, and C. S. Barnes. Binary Decision Clustering for Neural Network Based Optical Character Recognition. *Pattern Recognition*, 29(3):425–437, 1996.

[8] C.S. Weaver and J.W. Goodman. Technique for optically convolving two functions. *Appl. Opt.*, 5:1248–1249, 1966.

[9] F.T.S. Yu and X.J. Lu. A real-time programmable joint transform correlator. *Opt. Commun.*, 52:10–16, 1984.

[10] J.L. Horner. Optical processing or security and anticounterfieting. *IEEE LEOS=9296 Proceedings, Boston, 18-21 November*, 1:228–229, 1996.

[11] Y. Petillot, L. Guibert, and J.-L. de Bougrenet de la Tocnaye. Fingerprint recognition using a partially rotation invariant composite filter in a FLC joint transform correlator. *Opt. Comm.*, 126:213–219, 1996.

[12] J. Podolfo, H. Rajenbach, and J-P Huignard. Performance of a photorefractive joint transform correlator for fingerprint identification. *Opt. Eng.*, 34:1166–1171, 1995.

[13] B. Javidi and J. Wang. Position-invariant two-dimensional image correlation using a one-dimensional space integrating optical processor: application to security verification. *Opt. Eng.*, 35:2479–2486, 1966.

[14] T.J. Grycewicz and B. Javidi. Experimental comparison of bianry joint transform correlators used for fingerprint identification. *Opt. Eng.*, 35:2519–2525, 1996.

[15] F.T. Gamble, L.M. Frye, and D.R. Grieser. Real-time fingerprint verification system. *Appl. Opt.*, 31:652–655, 1992.

[16] K.H. Fielding, J.L. Horner, and C.K. Makekau. Optical fingerprint identification by binary joint transform correlation. *Ope. Eng.*, 30:1958–1961, 1991.

[17] J.L. Horner and H.O. Bartelt. Two-bit correlation. *Appl. Opt.*, 24:2889–2893, 1985.

[18] D. Psaltis, E.G. Pack, and S.S. Venkatesh. Optical image correlation with a binary spatial light modulator. *Opt. Eng.*, 23:698–704, 1984.

[19] D. F. Specht. Probabilistic neural networks. *Neural Networks*, 3(1):109–118, 1990.

[20] O. M. Omidvar and C. L. Wilson. Information Content in Neural Net Optimization. *Journal of Connection Science*, 6:91–103, 1993.

[21] J. L. Blue and P. J. Grother. Training Feed Forward Networks Using Conjugate Gradients. In *Conference on Character Recognition and Digitizer Technologies*, volume 1661, pages 179–190, San Jose, February 1992. SPIE.

[22] P. J. Grother. Cross Validation Comparison of NIST OCR Databases. In D. P. D'Amato, editor, , volume 1906, pages 296–307, San Jose, 1993. SPIE.